

## **II.C Enabling Technologies**

### **II.C.1 NO<sub>x</sub> Sensor for Direct Injection Emission Control**

*David B. Quinn (Primary Contact), Earl W. Lankheet (Principal Investigator)*  
*Delphi Corporation*  
*MC 485-220-065*  
*1601 N. Averill Ave.*  
*Flint, MI 48556*

*DOE Technology Development Manager: Roland Gravel*

*Subcontractor:*  
*Electricore, Inc., Indianapolis, IN*

#### **Objectives**

- Develop an electronics control circuit for the NO<sub>x</sub> sensor.
- Develop the packaging for the electronic controller (on hold due to project limitations).
- Develop the sensing element structure based on integrating zirconia and alumina ceramics and planar element technology.
- Develop the interconnection method to carry power and signal to and from the NO<sub>x</sub> measurement device.
- Develop the necessary materials and process refinements in support of the ceramic sense element.

#### **Approach**

- Use alumina and zirconia ceramic tapes and thick film screen-printed pastes to form the necessary control and measurement cells. Integrate the heater on the co-fired substrate.
- Initiate development using simple configuration test samples and coupons. Continue to evolve the design and test samples into a fully functional NO<sub>x</sub> measurement sense element.
- Confirm the operation of the sense element using bench and engine testing.
- Use Set Based Concurrent Engineering to develop alternative techniques to interconnect the power and signal wires to the sense element substrate. Use accelerated engine and environmental testing to establish the optimum interconnection approach.
- Use existing sensor packaging technology to house and protect the sense element.

#### **Accomplishments**

- Transitioned to a new source of ceramic green tape and modified the production process to accommodate its unique features.
- Successfully passed hot vibration and shock testing equivalent to 200,000 miles of vehicle operation.
- Demonstrated comparable signal measurement for both oxygen and NO<sub>x</sub> signals to a NO<sub>x</sub> reference sensor on a diesel engine dynamometer.
- Demonstrated functional performance of a NO<sub>x</sub> sensor with over 10,000 vehicle miles accumulated.
- Made significant design and materials improvements.
- A Gen II electronic controller was developed that incorporates electronic hardware and software improvements.

## Future Directions (4-month project extension)

- Test sensors and Gen II controllers and report data.
- Write final report.

---

## Introduction

This project is developing the remaining technologies needed to deliver a robust NO<sub>x</sub> sensor for use in closed-loop control of NO<sub>x</sub> emissions in lean-burn engines such as compression ignition direct injection engines. At least two applications for NO<sub>x</sub> sensors have been identified: (1) for engine-out control of NO<sub>x</sub>, requiring a range of zero to 1500 ppm; and (2) for aftertreatment control and diagnostics, requiring a range of less than about 100 ppm NO<sub>x</sub>.

This activity builds on existing and developing Delphi technology in multi-layer and exhaust sensor ceramics.

## Approach

The Delphi-led team continues to develop the electrochemical planar sensor technology that has produced stoichiometric planar and wide-range oxygen sensors as the basis for development of a NO<sub>x</sub> sensor. Zirconia cell technology with an integrated heater will provide the foundation for the sensor structure. Proven materials and packaging technology will help to ensure a cost-effective approach to the manufacture of this sensor.

The electronics technique and interface are considered to be areas where new strategies need to be employed to produce higher signal-to-noise ratios of the NO<sub>x</sub> signal with emphasis on signal stability over time for robustness and durability. Both continuous mode and pulse mode control techniques are being evaluated.

Packaging the electronics requires careful design and circuit partitioning so that only the necessary signal conditioning electronics are coupled directly in the wiring harness, while the remainder are situated within the electronic control module for durability and costs reasons. This task continues to be on hold due to the limitation that definition of the interface electronics was unavailable until very late in the project.

The sense element is based on the amperometric method utilizing integrated alumina and zirconia ceramics. Precious metal electrodes are used to form the integrated heater, as well as the cell electrodes and leads. Inside the actual sense cell structure, it is first necessary to separate NO<sub>x</sub> from the remaining oxygen constituents of the exhaust, without reducing the NO<sub>x</sub>. Once separated, the NO<sub>x</sub> will be measured using a measurement cell. Development or test coupons have been used to facilitate material selection and refinement, as well as cell, diffusion barrier, and chamber development.

The sense element currently requires elaborate interconnections. To facilitate a robust, durable connection, mechanical as well as metallurgical connections are under investigation. Materials and process refinements continue to play an important role in the development of the sensor.

## Results

The sense element of the NO<sub>x</sub> sensor is comprised of multiple ceramic layers of alumina and zirconia ceramics. These layers have features, e.g., electrodes, leads, heater serpentine, diffusion channels, etc., printed on them to ultimately form the design of the sense element. The printed layers are “stacked” appropriately, laminated and then cut to form individual sense elements prior to sintering. There is a great deal of ceramic and thick film design and processing expertise required to form the complex features of the NO<sub>x</sub> sensor. Sintered NO<sub>x</sub> sense elements are illustrated in Figure 1.

At the beginning of this fiscal year of the project, there was a need to switch to a new supplier for the green ceramic tapes. The original source was discontinuing supply. The move to the new source of tape was successful after several tape lots and trial sense element builds were made. A number of processing parameter adjustments were identified and carried out to enable the successful transition to the new tape source. A substantial quantity of NO<sub>x</sub>

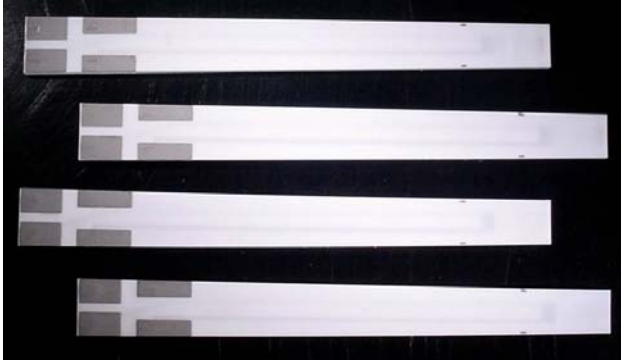


**Figure 1.** NOx Sense Elements Fabricated from New Source of Ceramic Tape

sense elements was fabricated and sintered to ensure the new tape was capable.

A key part of the sensor technology requiring development is the interconnection of the sensor signal wires to the sense element contact pads. This connection needs to be robust to temperature, vibration, and shock and continue to maintain signal continuity. The interconnection technique for the NOx sensor is more difficult due to the limited space available to make a connection to the eight contact pads. Various connection techniques were evaluated, including mechanical, brazing, welding, etc. In the end, the mechanical connection technique was selected and further developed due to its ease of manufacturability and overall cost.

A critical test for the interconnection and overall package is a vibration and shock test. This severe test comprises cycling the exhaust temperature from about 150°C to about 950°C, while running 2-axis vibration (sine wave and random) simultaneously. The accelerated test is meant to simulate 200,000 miles of vehicle/engine conditions. Figure 2 shows a typical vibration and shock test at the high temperature condition where glowing exhaust pipes can be seen. Five sensors were tested for hot vibration and shock, with all of the interconnections maintaining continuity throughout the test.

Fully functional sensors with Gen I electronic controllers were characterized on a gas bench, calibrated and then run on a diesel engine dynamometer. Sensors were located in both engine-out and post-catalyst positions, as shown in Figure 3.

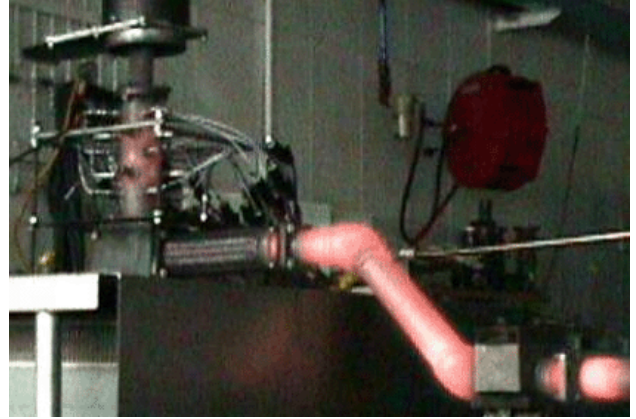


**Figure 2.** Hot Vibration and Shock Test Showing Hot Cycle

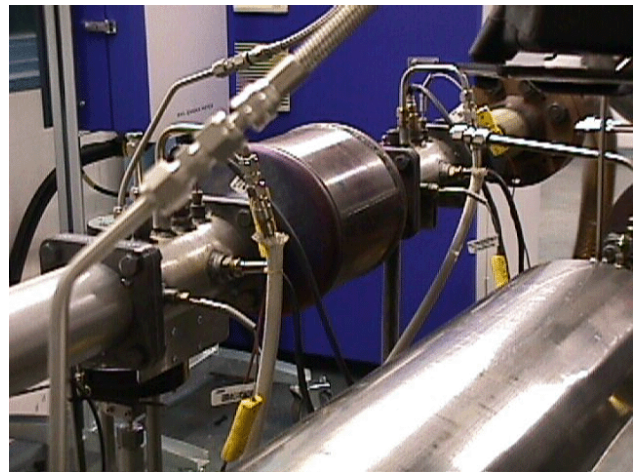


**Figure 3.** Diesel Engine Dynamometer Test Site Showing Engine-Out and Post-Catalyst Locations

Both the oxygen and NOx signals were recorded and compared with a competitive sensor. The sensors were evaluated using a thirteen-step mode driving cycle. Figure 4 compares the oxygen signal from the Delphi sensor with a reference sensor's oxygen signal over the twenty-eight minute test. The two signals are essentially identical throughout the entire test. The NOx signal was also compared to a reference sensor and is shown in Figure 5. Overall, there is good general agreement between the two sensors, but there are times when the Delphi sensor reports higher NOx than the reference sensor and other conditions when lower NOx is reported. This activity sponsored a more detailed study of accuracy of the sensor. A closer review of the engine data

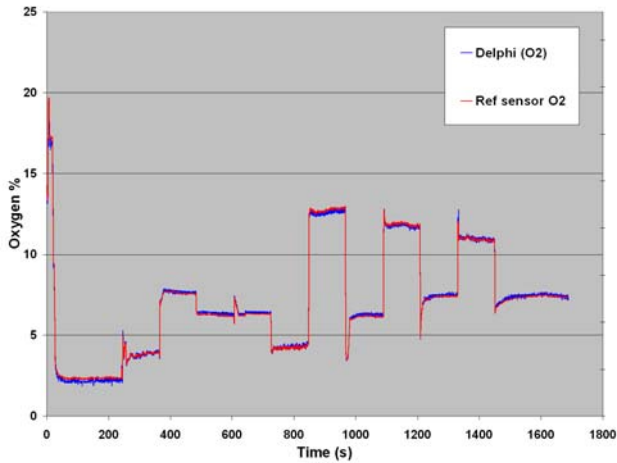


Figure 4. Oxygen Measurement versus NOx Reference Sensor Oxygen Signal

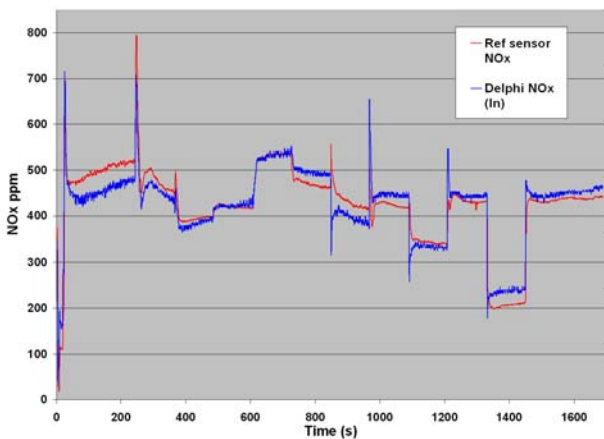


Figure 5. NOx Measurement versus NOx Reference Sensor

illustrates that the Delphi sensor seems to have a faster response.

A NOx sensor was also placed on a diesel passenger car to accumulate typical road miles. The sensor was characterized before installation on the vehicle and from time to time as mileage accumulated. The first sensor and controller system accumulated over 7500 miles before it was decided to upgrade to more current hardware levels of the sensor and controller. The second system has been on the vehicle for over 10,000 miles with the sensor still functional. Figure 6 shows the original gas bench NOx output versus the output after 10,000 miles on the vehicle. Although the output appears to have “shifted” down, the slopes of the two curves are

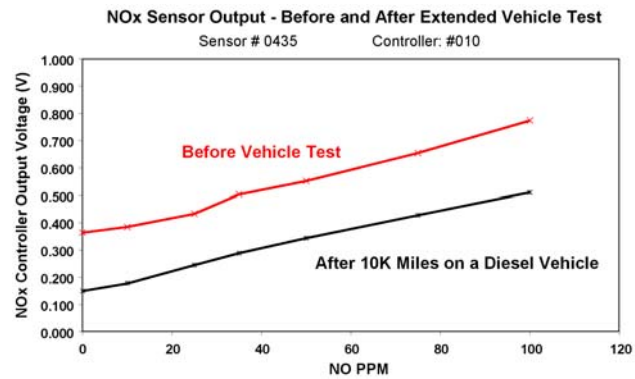


Figure 6. NOx Sensor Output Curve Before and After 10,000 Vehicle Miles

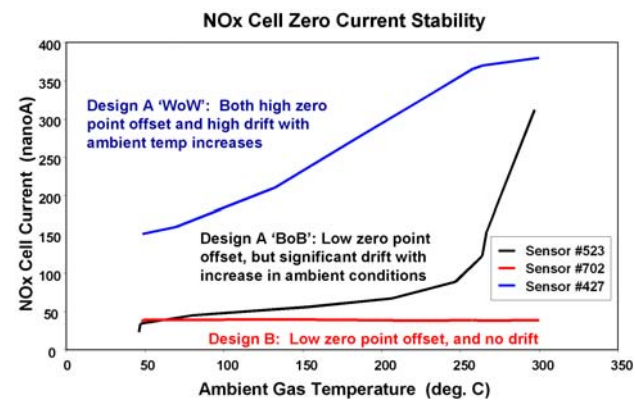


Figure 7. NOx Cell Zero Point Current Stability versus Temperature

identical, with no loss in gain of the signal. The cause of this change in output is under investigation.

NOx sensors were characterized on a gas bench to determine causes for inaccuracies in the area of 0 to 25 ppm NOx. One of the largest areas of error was found to be related to a zero point offset. The offset at 0 ppm NOx has ranged from about 125 nanoAmps to as much as 800 nanoAmps on some sense elements. A root cause analysis of the elements was made and a major cause of error was found relating to the structure of the element. It was also determined that the error grew in significance with an increase in ambient temperature, as shown in Figure 7 (Sensor design A – Worst of the Worst “WoW” and Best of the Best “BoB”). Sensor design A represented a typical NOx sense element for the mid-2005 period. Sensor design A “WoW” shows a zero point offset of roughly 150 nanoAmps at room

temperature, and as the exhaust gas temperature is increased, it more than doubles the output. Sensor design A “BoB” was derived from a sort process and has both a lower room temperature zero point offset and a less dramatic increase in output with temperature until about 250°C, where there is a large increase in output with increasing temperature. Sensor design B incorporated a number of materials and design modifications which were meant to increase the stability of the sensor output versus temperature. The sensor does have a low zero point offset at room temperature, and it shows excellent stability throughout the ambient gas temperature range tested. These modifications will become part of the standard design going forward.

Figure 8 illustrates the Gen II controller. This controller represents the next generation of control for the NOx sensor. It has both hardware and software improvements. It is meant to be a controller capable of supporting prototype testing across vehicle, bench, or dynamometer. The controller has evolved from a three-circuit board design to a single board. A new microprocessor was implemented that has re-useable software architecture. The controller has an additional Controller Area Network channel to support instrumentation and vehicle needs concurrently. Additional improvements have been made to the heater warm-up routine and cell control techniques. The sampling rate was increased for temperature feedback, to allow for better control during transient conditions. Other improvements include lower noise in the output signal as well as improvements in cell diagnostics.

### **Conclusions**

The mechanical system that connects the sensor element to the housing was tested for robustness using a hot vibration and shock dynamometer test. Results indicated that the design concept shows the potential to survive an equivalent of 200,000 miles of vibration and shock. This would be a significant achievement for a ceramic-based exhaust sensor with 8 interconnects.



**Figure 8.** Gen II NOx Sensor Electronic Controller

NOx sensors and controllers were tested on a diesel engine dynamometer with both the oxygen and NOx signals comparing favorably with the signals of a NOx reference sensor. Some offsets in the NOx signal were observed and are part of an ongoing accuracy study as Delphi continues efforts to develop this technology.

Improvements to the zero point offset of the NOx signal were made through sensor materials and design modifications. The zero point and thus the NOx measurement are now much more stable with ambient gas temperature changes.

Gen II controllers incorporating electronic hardware and software design improvements were built and tested and are ready for integration with NOx sensors. Delphi still envisions significant development effort on sensor interface electronics to support robust sensor output.

## II.C.2 Small, Inexpensive Combined NO<sub>x</sub> and O<sub>2</sub> Sensor

*W. N. Lawless, C. F. Clark (Primary Contact)*

*CeramPhysics, Inc.*

*921 Eastwind Drive, Suite 110*

*Westerville, Ohio 43081*

*DOE Technology Development Manager: Roland Gravel*

*Subcontractors:*

*MRA Laboratories, Adams, MA*

*RJS Electronics, Columbus, OH*

### Objectives

- Demonstrate a miniature, amperometric, inexpensive NO<sub>x</sub> sensor body in the form of a multilayer ceramic capacitor.
- Incorporate NO<sub>x</sub> sensor body with a similar oxygen sensor body in a zirconia tube as a fully assembled NO<sub>x</sub> sensor.
- Demonstrate microprocessor-based measuring electronics.
- Supply sensors and measuring electronics for testing at Rosemount Analytical and other outside institutions.

### Approach

- Measure NO<sub>x</sub> sensing characteristics of a matrix of sensor bodies manufactured from stabilized zirconia in the form of multilayer capacitors with porous, Rh-based electrodes.
- Determine optimum electrodes, operating temperature range, and long-term stability of NO<sub>x</sub> sensor bodies.
- Design and breadboard microprocessor-based measuring electronics and characterize.
- Prepare sensors and measuring electronics and supply these to Rosemount and others for testing.
- Develop shell of zirconia with diffusion barrier at one end, sealed at the other end. Oxygen will be pumped from the interior and NO<sub>x</sub> and the residual oxygen will be measured, allowing a calculation of NO<sub>x</sub> in the ambient gas.

### Accomplishments

- Capacitor-type sensor bodies successfully manufactured with a matrix of porous Rh-based electrodes varying in composition from 10/90 to 100/0 Rh/Pt ratio.
- Solved technical hurdle of rhodium oxidation.
- Large NO<sub>x</sub> sensitivity demonstrated with sensor bodies made of all variations of Rh-based electrodes.
- Operating temperature range and voltage determined.
- Measuring electronics designed, built and tested successfully.
- Zirconia shell and diffusion plug designed and under development.

### Future Directions

- Continue characterizations and long-term testing of NO<sub>x</sub> sensor body.
- Finish development of electronic control of partial oxygen pressure inside the assembled sensor and its temperature.

- Incorporate NOx and O<sub>2</sub> sensor bodies into fully assembled NOx sensors.
- Complete testing at outside institutions.

**Introduction**

The need exists for an inexpensive, reliable, on-board sensor to monitor NOx emissions of vehicles to meet state and federal regulations. This NOx sensor project builds on a recent successful project supported by DOE to develop a miniature, amperometric oxygen sensor manufactured from stabilized zirconia as a multilayer ceramic capacitor with porous Pt electrodes which catalyze oxygen molecules to oxygen ions. The basic concept of the oxygen (and NOx) sensor is illustrated in Figure 1. Oxygen ions are "pumped" from the (-) to the (+) electrodes across the zirconia ceramic layers under an applied voltage, and this amperometric current provides a measure of the oxygen partial pressure in the surrounding gas. The porosity of the Pt electrodes provides the necessary diffusion limitation, and there is no need for a reference gas. The sensitivity of this oxygen sensor is shown in Figure 2, and the output current is in the milliamp range. The sensor body contains eleven active ceramic layers and is approx. 2 mm x 3 mm x 5 mm. The established manufacturing methods for ceramic capacitors make this a very low-cost sensor body (~\$1).

It is well known that Rh catalyzes NOx to nitrogen and oxygen. If porous Rh electrodes are substituted for the porous Pt electrodes above, the resulting sensor will have an amperometric-current output due to the oxygen released from the NOx and

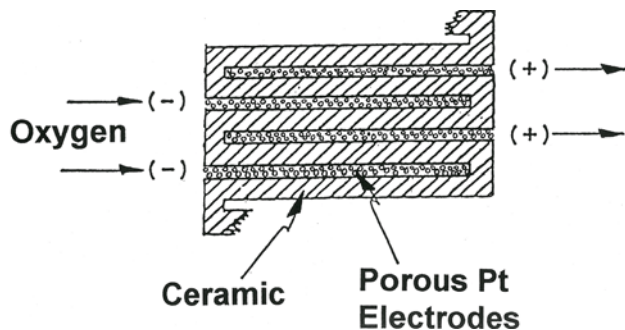


**Figure 1.** Schematic illustration of the capacitor-type amperometric sensor body showing the porous electrodes. The ceramic layers are stabilized zirconia and the electrodes are Pt in this example.

thereby provide a NOx measurement. A schematic illustration of a combined oxygen and NOx sensor is shown in Figure 3. The oxygen sensor is mounted in the open end of the zirconia tube to measure the oxygen in the exhaust gas, and bonded oxygen and NOx sensors are mounted in the closed end. Exhaust gas diffuses through a diffusion plug into the inner

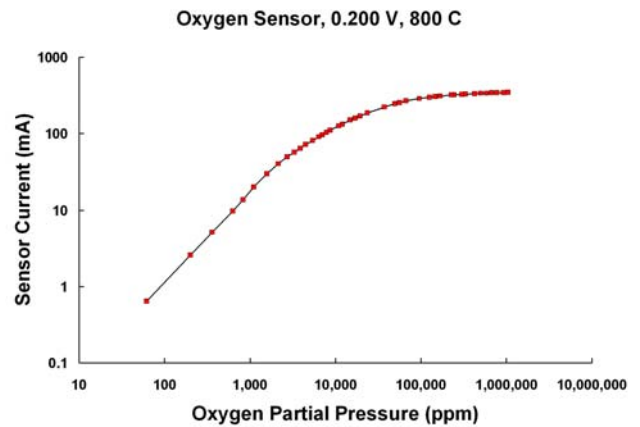


**Figure 2.** Oxygen sensitivity of the previously developed amperometric oxygen sensor (0.1 VDC applied).

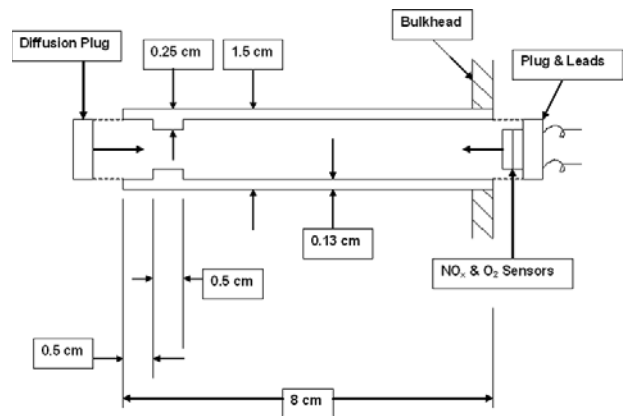


**Figure 3.** Schematic illustration of the combined sensor for measuring both the oxygen partial pressure and NOx content of an exhaust gas. The exhaust gas diffuses through the zirconia diffusion plug, and the oxygen level in the inner chamber is pumped to a small, residual level by applying a voltage to the Pt/Au cathode and Pt anode electrodes.

chamber, where the oxygen in the gas is pumped to a low, residual level by a voltage applied across the Pt anode and the Pt/Au cathode. The oxygen sensor measures only the oxygen content of the gas. The NOx sensor measures both the oxygen and NOx contents. The difference in these two measurements is then a measure of the NOx content of the exhaust gas. It is estimated that this combined sensor would be about 2.5 cm long, 1.3 cm in diameter, and parts cost would be \$5 – \$10.

**Approach and Results**

The capacitor manufacturer made zirconia sensor bodies with Rh electrodes and three active ceramic zirconia layers, 0.008 cm thick. The first step involved measuring the NOx sensitivity as a function of sintering temperature because, as with the oxygen sensor, the important porosity of the electrodes decreases with increasing sintering temperature. Sintering temperatures in the range 1175 - 1225°C were used, and the optimum temperature is 1200°C. The basic concept of sensing NOx was demonstrated in these tests.

However, a fundamental problem arose in that the Rh slowly oxidizes in the 600 - 800°C operating range, and the amperometric current degrades with time. As the oxidation goes to completion, the volume change causes the sensor body to delaminate. Therefore, the emphasis shifted to using Rh-Pt alloys for the electrodes to inhibit electrode oxidation, and the manufacturer made sensor bodies with a matrix of alloys 10%/90% and 75%/25% Rh/Pt electrodes. The alloying significantly decreases the rate of oxidation without affecting the NOx sensitivity. The rate of oxidation was measured by monitoring the change in resistance of the electrodes as a function of time at various temperatures. Typical results are shown in Figure 4, which is an Arrhenius plot of the change in resistance with time versus temperature. The 50%/50% Rh/Pt electrodes reduce the oxidation rate significantly compared to the pure Rh electrodes.

Typical NOx sensitivity is shown in Figure 5 as a function of the voltage applied to the sensor. In order to keep testing costs down, all these measurements have been made using sensor bodies with only three active layers (refer to Figure 1). The final sensor bodies will have up to 30 electrodes, which will

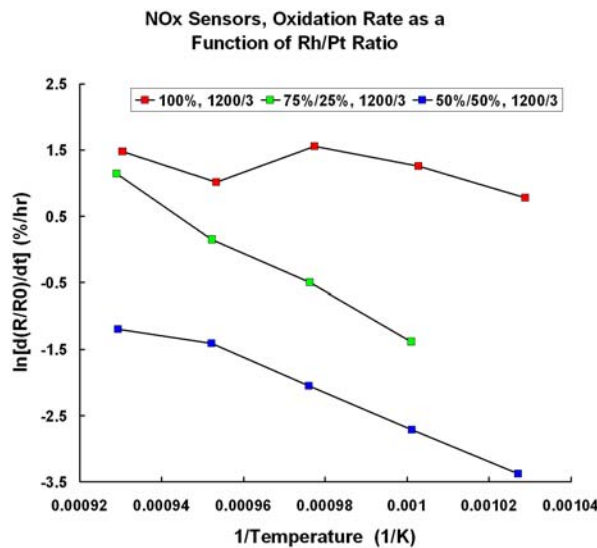


**Figure 4.** Arrhenius plot of the rate of change of resistance versus temperature for various electrode alloy materials.

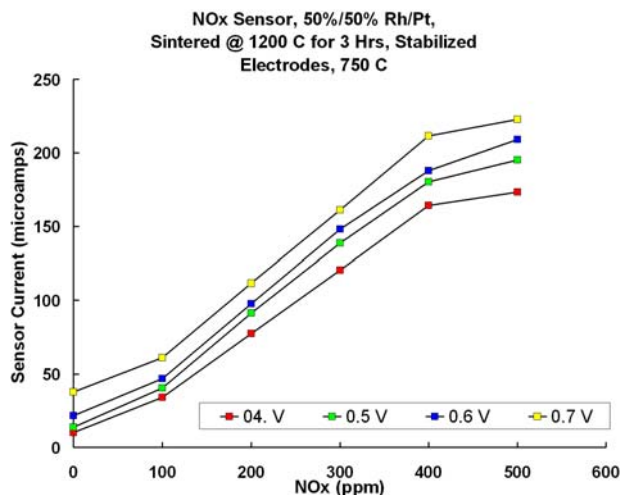


**Figure 5.** Typical NOx sensitivity curves for NOx sensor bodies with three electrodes and 50%/50% Rh/Pt electrodes as a function of applied voltage.

increase the response shown in Figure 5 by a factor of ten.

The basic electronic hardware has been designed, built, and tested successfully. This instrument has three outputs for each of the three sensors shown in Figure 3. Each output holds the voltage constant at the sensor while providing for independent measurement of the current through that sensor. In addition, a separate controller for regulating the

temperature of the zirconia shell and the oxygen content inside the shell has been built and is currently being tested.

### **Conclusions**

The basic concept of a miniature, inexpensive, amperometric NOx sensor *has been demonstrated*, and this is the *key* element in the combined oxygen and NOx sensor illustrated in Figure 3. (The accompanying oxygen sensor was developed previously). The prospect of achieving a small, inexpensive NOx + oxygen sensor that does not require a reference gas is now very promising, and such a sensor would serve an important diagnostic function onboard trucks and other vehicles for emissions control.

### **Patents**

1. Patents have issued for the Oxygen Sensor (US 6,592,731), and the NOx Sensor (Combined Oxygen and NOx Sensor, No. 6,824,661 B2). Both patents were based on patent disclosures filed with the Patent Office prior to the receipt of the corresponding DOE contract.

## II.C.3 Particulate Matter Sensor for Diesel Engine Soot Control

*Michael Rhodes*

*Honeywell Inc.*

*MN65-2700*

*3660 Technology Drive*

*Minneapolis, MN 55418*

*DOE Technology Development Manager: Roland Gravel*

*NETL Project Manager: Carl Maronde*

*Subcontractors:*

*University of Minnesota, Minneapolis, MN*

*Honeywell Control Products, Freeport, IL*

### Objectives

- To develop diesel engine exhaust particulate matter (PM) sensor prototypes that have low cost, high speed, reliability, and are capable of operating directly in the harsh exhaust of a diesel engine.
- Install the sensor prototypes in an appropriate engine test and compare test results to results of other reference instrumentation.
- Use test results to improve sensor concepts and to develop compatible sensor packages.
- Develop associated sensing electronics and signal processing hardware.
- Demonstrate prototype sensor to the DOE.

### Approach

The project has three main steps in order to accomplish the research:

- **PM Sensor Development**—Design and build several prototypes of PM sensors utilizing high-temperature materials for operation directly in the exhaust stream. Honeywell will develop different readout electronic circuits to monitor the sensor and interface to data acquisition equipment and/or engine controllers.
- **Sensor Testing**—Establish a diesel engine test bed that will include reference particulate measuring instrumentation and potentially other gas sensing instrumentation. A data acquisition system will be established that will be used to record the testing results for further data analysis. These tests will be conducted at the University of Minnesota's Center for Diesel Research and will utilize equipment from their Particle Measurement Laboratory. Gas concentration and particle size distribution information will be recorded to compare to sensor test results.
- **Sensor Packaging**—Staff members of Honeywell Labs and Sensing and Controls Division will develop suitable sensor packages for the PM sensors. Packaging materials should provide protection to the sensor as well as the ability to withstand the harsh operational environment. Sensor packages will be exposed to high temperatures and corrosive and potentially condensing environments. Destructive and nondestructive testing of the sensor package will be completed.

### Major Accomplishments to Date

- We have tested developed prototypes at the test facilities at the University of Minnesota using three commercial diesel engines. The first is a John Deere 4540T engine typical of medium-duty off-road applications, the second is a Caterpillar engine typical of heavy-duty on-road applications, and the third is a Volkswagen TDI (Euro IV) engine typical of passenger car applications.

- We have established the feasibility of monitoring the particulates directly in the exhaust manifold without pretreatment or dilution and without sensor fouling due to accumulation of PM.
- We have demonstrated the feasibility of monitoring particulates from each combustion event in real-time on a cylinder-by-cylinder basis.
- We have correlated these cylinder-by-cylinder and cycle-by-cycle variations to engine operating parameters such as fuel injection variability and exhaust gas recirculation (EGR) behavior.
- Prototype devices have been fabricated for testing at end-user facilities.
- Preliminary optimization of the probe design has been done to improve the signal response.
- Amplifier electronics have been developed to provide signal detection as a replacement for the laboratory charge amplifier.
- Signal processing methods have been developed to establish the particulate-related signal from the total engine exhaust signal. These methods use analysis in the frequency domain to provide noise reduction.
- We have tested developed prototypes at two user facilities external to the University of Minnesota – Oak Ridge National Laboratory (ORNL) and Cummins.

---

## **Introduction**

Emission regulations worldwide emphasize reducing fine particulate matter emissions. Recent studies have shown that fine particles are more strongly linked with adverse health effects than are larger particles, and engines are an important source of fine particles.

Particles in the nucleation mode and in the accumulation phase appear to be formed by different mechanisms. Accumulation mode particles are primarily carbonaceous and are associated with rich combustion and poor subsequent oxidation during the engine cycle. Most nucleation mode particles are not even formed until the exhaust dilutes and cools. They consist of a complex, poorly understood mix of sulfuric acid and partially burned fuel and lubricating oil. Formation of these two types of particles likely occurs under different engine operating conditions, with:

- Heavy loads favoring carbonaceous accumulation mode particles, and
- Light loads most likely favoring the formation of vapor phase precursors of nucleation mode particles. These precursors may not undergo gas-to-particle conversion until the exhaust cools and dilutes in the atmosphere.

In order to meet future emission standards, future diesel engines will have to be fitted with sophisticated combustion control systems and, almost certainly, an after-treatment system including

particle filters or traps. An effective exhaust particulate sensor would not only lead to a reduction of particulate emissions from the engine itself, but would also make traps and other after-treatment devices more feasible. Particulate traps are now commercially available and are likely to be applied in high volume in the future. They are large, expensive and impose a significant fuel economy penalty. The particulate sensor would help reduce the amount of particulate matter created through better engine control. It could also be used to monitor particulate loading or breakthrough on downstream traps. Thus, the particulate trap could potentially be made smaller or be regenerated less often.

## **Results**

### **Sensor Testing**

Initial testing of the sensors at user facilities determined that there was significant noise in the sensor signal due to 60 Hz noise found at the various facilities and also signal variations that were not readily identifiable. A Honeywell-funded sensor recovery project was initiated to determine these noise issues with measurements for microphonic noise, electronic noise, and noise due to any sensor vibration. During the testing of sensor vibration noise, a ball was placed at the end of the sensor probe to try and induce additional vibration to the sensor and to see if any component of that vibration was due to pressure or velocity variances in the exhaust stream. No additional noise due to vibration was

seen, but the signal amplitude increased by about 50% due to the increased surface area. The revised probe is shown in Figure 1.

The signal processing changes indicated that, using frequency analysis, the signal due to particles could be extracted from the raw engine exhaust signal. The processed signal is proportional to the carbon-black particle concentration. To determine the signal proportionality, testing was done at the University of Minnesota to relate the sensor response to the particle concentration. Figure 2 indicates the correlation of the sensor signal to a fast-response aetholometer. This testing has shown that the sensor is capable of responding to particle mass concentrations down to below  $2 \text{ mg/m}^3$ .



Figure 1. New Honeywell PM Sensor Probe Based On Improved Signal Tests

The sensor testing was also conducted at different loads and engine operating speeds. The sensor was found to respond to the particle concentrations produced during changes in engine loading and speed.

The testing at Cummins indicated that the PM sensor gave time-responsive results that followed the engine conditions and also followed the opacity meter being used by Cummins for the smoke measurements. The testing not only included operating the engine at different smoke conditions, but also operating the engine in an acceleration and deceleration throttling mode (rapidly opening and closing the throttle). As shown in Figure 3, the sensor was able to follow these rapid changes well. In addition, the processed sensor data did not respond to 60 Hz noise (of which there was a considerable amount) and showed very little effect of changing engine speed (which was one of the results also desired by Cummins). Figure 3 indicates how the sensor responded when the engine was run under constant rpm and load conditions and the smoke levels were changed by adjusting the timing. The smoke levels were taken from around 1.5% opacity up to 15% and then reduced back to 1.5% again. Cummins mentioned that the opacity measurements were within the testing conditions usually conducted by Cummins.

The testing at ORNL used a newer Deere 4045 engine. The PM sensor was placed about 6 ft downstream of the turbo, and a sensor probe 3.5 inches in length was used. The ORNL particle

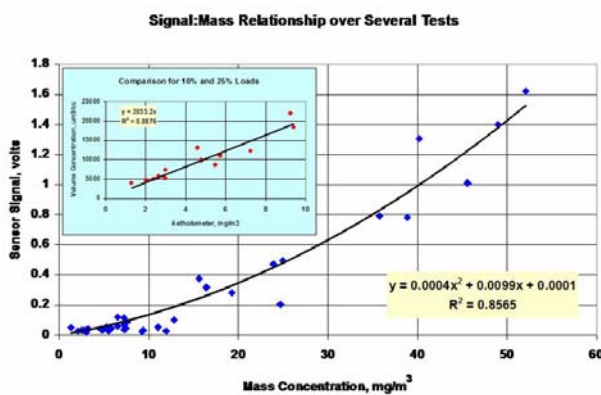


Figure 2. Correlation of Sensor Signal to Black Carbon Concentration as Measured with a Reference Fast-Response Aetholometer

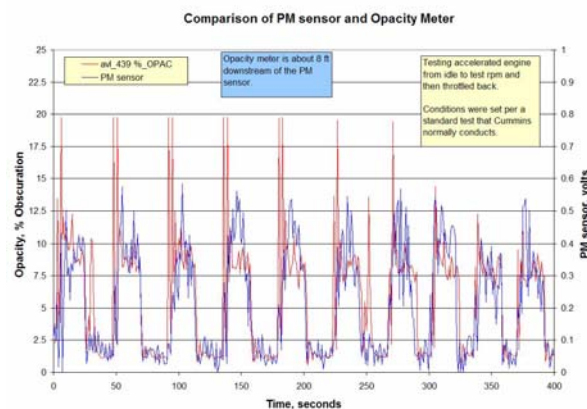


Figure 3. Comparison of Sensor Signal with Opacity Signal during Engine Changes

instrumentation used included a scanning mobility particle scanner (integrated mass measurements were made) and smoke meter (Bosch) located about 4-5 feet upstream of the PM sensor.

Tests were conducted at a constant speed and load, and the rail pressure was adjusted to modify the smoke concentration. The tests that were conducted and the smoke numbers obtained are shown below:

- 1400 rpm, 300 ft-lb, 75 MPa rail pressure, smoke number – 0.26-0.29
- 1400 rpm, 300 ft-lb, 100 MPa rail pressure, smoke number – 0.13
- 1400 rpm, 300 ft-lb, 125 MPa rail pressure, smoke number – 0.12
- 1400 rpm, 300 ft-lb, decreased rail to 50 MPa, smoke number – 0.71

The comparison of the sensor signals against smoke number is shown in Figure 4.

These first tests changed the rail pressure from 50 to 125 MPa. The smoke number decreases with increased rail pressure in what appears to be a non-linear manner. The PM sensor output also decreases with increasing rail pressure. The PM sensor output at 50 MPa was around 0.4, which may have been due to some electronics clipping at these conditions. This effect needs to be evaluated.

The PM sensor was found to be a little noisier at the low smoke numbers. Part of the reason may be the pacification that is occurring with the sensor electrode since no conditioning was done before testing the sensors. Several other conditions were checked during the testing. One of these was the

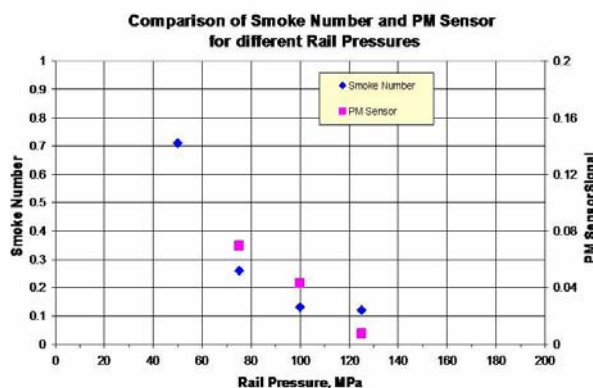


**Figure 4.** Sensor Signal and Smoke Number against Different Rail Pressures

difference between data observed from the 15-20 Hz and 35-50 Hz frequency bands from the signal processing. It was noted that during the testing, there were signal peaks at about 23 Hz and 45 Hz from the signal processing. This indicates the noise of the sensor as well as the difference in the signals at the two frequency bands. One factor to consider here is that since the sensor responds so rapidly, these signal variations could actually be variations in the exhaust particle concentrations. This will need to be evaluated in the future to determine signal optimization.

### Summary

Considerable technical progress has been made during FY 2005:

- Conducted sensor testing to determine different noise generation mechanisms. Developed sensor signal processing to eliminate noise and optimize sensor signal.
- Developed electronics for signal amplification for the sensor probe, which replaces the laboratory charge amplifier and produces a usable output voltage.
- Developed signal processing software to extract the required signal relating to particle mass from the raw exhaust signal. This signal processing also extracts 60 Hz noise from the signal.
- The sensor has been tested at both the Cummins and ORNL facilities. These tests have shown that the sensor response compares to smoke number and also to rapid response instrumentation such as an opacity meter.

### Conclusions

- The Cummins testing indicates that there is fairly good comparison between the opacity meter and the PM sensor. There are still some noise issues with the sensor that need to be addressed by the signal processing software. What is unknown is how much of this noise in the PM signal is really noise of the engine and exhaust conditions and how much is just noise in the signal.
- The testing at ORNL indicated that there is a definable relationship between smoke number and sensor signal. In addition, there is a relationship between the sensor and the smoke number for the process where fuel is injected after top dead center.

## II.C.4 Variable Compression Ratio Engine

*Charles Mendler*

*Envera LLC*

*7 Millside Lane*

*Mill Valley, California 94941*

*DOE Technology Development Manager: Roland Gravel*

*ORNL Project Managers: Norberto Domingo and Bruce Bunting*

### Objective

- Design and build a variable compression ratio (VCR) variant of the Mercedes-Benz 4-cylinder common-rail turbocharged compression ignition, direct injection (CIDI) engine.
- Incorporate second-generation VCR subsystems into the 4-cylinder VCR Mercedes CIDI engine.
- Provide VCR hardware that supports control of CIDI and spark ignition (SI) homogeneous charge compression ignition (HCCI) combustion.

### Approach

- Design/build of a VCR CIDI engine applying design optimization computer models and prior hardware build analysis and data.

### Accomplishments

- The Envera VCR mechanism was successfully packaged into an in-line 4-cylinder CIDI engine, demonstrating the manufacturing feasibility of VCR variants of production engines.
- Second-generation VCR components have been successfully designed and are currently being built, including a small profile crankshaft cradle, lubrication system, oil sealing system, actuator mechanism, and chain drive.
- Additional patents have been allowed and will be announced when publication dates become available.
- Dynamometer testing indicated that increasing compression ratio may reduce engine-out emissions from gasoline engines at part-load at engine speeds below 3000 rpm. VCR may provide cold-start and warm-engine emission benefits for spark ignition engines. Further testing is required to assess these benefits.

### Future Directions

- Demonstrate CIDI emissions, fuel economy, and advanced combustion benefits with VCR using the new Oak Ridge National Laboratory (ORNL) Mercedes VCR 1.7L 4-cylinder common-rail turbo-diesel engine.
- Demonstrate a fast-response VCR actuator system capable of supporting HCCI combustion. This project has been initiated with the DOE National Energy Technology Laboratory (NETL) and includes a gasoline 4-cylinder VCR engine. The most advanced VCR configuration is code-named G4.
- Investigate through dynamometer testing the potential for reducing cold-start and warm-engine emissions in gasoline engines using VCR.
- Demonstrate through testing and computer modeling the ability to attain controlled HCCI combustion using robust low-cost hardware.
- Demonstrate through testing and computer modeling the ability to attain 30 percent improvement in fuel economy with VCR concurrent with an increase in vehicle performance, and at significantly lower production cost than hybrid electric vehicle (HEV) technology.

## Introduction

Several VCR mechanism concepts have been advanced since U.S. Patent Number 5,819,702 was issued to Charles Mendler in 1998 and SAAB disclosed its VCR engine [1,2,3,4,5,6,7,8]. Since then, research conducted by the U.S. Department of Energy, the European Commission – Research, automobile manufacturers, and engine engineering firms has found that fuel economy can be improved by about 30% with VCR, boosting and engine down-sizing [3,4,9,10]. VCR may also enable or aid HCCI combustion, which would provide further gains in economy as well as reductions in diesel engine emissions. GM and others estimate that HCCI combustion offers the potential for improving gasoline fuel economy by about 25% [11].

Analysis has indicated that the fuel economy benefits of hybrid vehicles, advanced diesel engines and VCR are similar for vehicles of similar weight and power [2,4,12]. The 2006 Honda Accord hybrid may attain higher efficiency than earlier hybrids; however, some of the benefit may be due to engine improvements [13]. These powertrain types can be expected to coexist, where each option has market segment advantages. The primary advantages of VCR are low cost, high power, and U.S. emissions compliance.

Several VCR mechanisms have now been proposed and prototyped with U.S. and European government funding in addition to funding from automotive and diesel manufacturers and engine research firms. The Envera VCR mechanism remains a leading production candidate.

The first high-performance Envera VCR mechanism was built for the former Partnership for a New Generation of Vehicles (PNGV) program. The engine attained efficiency goals and continues to be used for research at ORNL. The latest-generation Envera VCR mechanism is about 75% lighter than first-generation PNGV hardware, can be packaged inside the oil pan of existing engine blocks, and has robust valve chain and power take-off systems.

The valve chain drive is shown in Figure 1. Table 1 shows selected data for the VCR CIDI engine. Because of patent interests, the full VCR

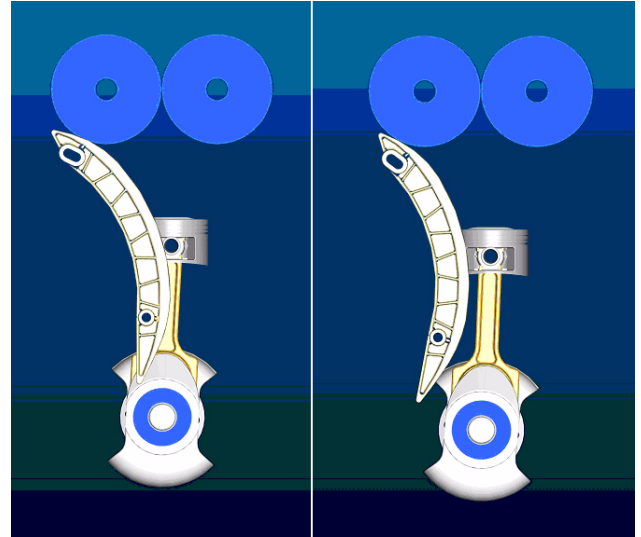


Figure 1. Envera VCR chain drive

Table 1. VCR 4-Cylinder CIDI Engine Specifications

Cylinders	4
Valves per cylinder	4
Valve actuation	DOHC Roller finger followers with hydraulic lash
Bore spacing	90 mm
Bore	80 mm
Stroke	84 mm
Bore/stroke ratio	0.95
Displacement	1.689 L
Compression ratio	18:1 maximum 9:1 minimum
Fuel injection	Common rail
Cold-start	Glow plug
Boosting	Turbocharged

system cannot be disclosed. The attached pictures are of the chain drive at high and low compression ratio (CR) values. The lower chain guide pin is mounted to the VCR eccentric, and the upper pin to the engine block. The pivoting motion of the chain guide maintains a constant chain pathway length at all CR values. The zero-cost solution is elegant in its simplicity. VCR technology can cost thousands of dollars less per car than hybrid technology. VCR

technology also provides significant increases in power. For these two reasons, VCR technology can be expected to capture market share.

**Approach**

The 4-cylinder VCR turbo-CIDI engine is currently being built. Design optimization computer models, prior analysis, and data were used in the current project. Resources used for the project include:

ProEngineer Wildfire 2.0	Part and mechanism assembly
Internal data file	Master Tracker of specifications
Subcontracted	Finite element analysis
MDO Extension	Dynamic force analysis
GTPower	Gas force on the piston
Origin 7.5	Data conversion
Subcontracted	Quick-cast rapid prototyping
Subcontracted	CNC machining

**Results**

All-new VCR subsystems enhance commercial prospects of the Envera VCR mechanism, including a small profile crankshaft cradle, lubrication system, oil sealing system, actuator mechanism, power take-off and chain drive.

The VCR common-rail turbo-CIDI engine will be a valuable tool for ORNL in conducting research on emissions reduction, efficiency gains, and advanced combustion/HCCI.

**Conclusion**

A second-generation Envera VCR engine is being built for ORNL. The CIDI engine includes all-new VCR subsystems that enhance commercial prospects for the technology. Significant national oil savings could be realized with the VCR technology due to its low cost and sizable efficiency benefits. Reduced cylinder count with VCR and boosting can improve fuel economy by about 30%. The efficiency of the VCR engines could be further improved by HCCI combustion as that technology matures. The

VCR technology can be integrated into production engines and has a significantly lower cost than HEV technology.

**Patents**

1. Additional patents have been allowed and will be announced when publication dates become available.

**References**

1. Mendler, Charles (ENVERA): High Efficiency Vehicle and Engine, US Patent Number 5,819,702, October 13, 1998.
2. Drangel, H., Olofsson, E., and Reinmann, R. (SAAB): Variable Compression (SVC) and the Combustion Control (SCC) – Two Ways to Improve Fuel Economy and Still Comply with World-Wide Emissions Requirements, SAE Paper 2002-01-0996, 2002.
3. Automotive Engineering International (SAAB), pages 54-57, SAE, April 2001.
4. Automotive Engineer (SAAB), page 36, December 2000.
5. FEV Spectrum, Issue 22, February 2003.
6. Yapici, K. I. (FEV), US Patent Number 6,588,384 B2, July 8, 2003.
7. Moteki, K. et al. (NISSAN): A study of a Variable Compression Ratio System with Multi-Link Mechanism, SAE paper 2003-01-0921, 2003.
8. Automotive Engineering International (NISSAN), pages 76-78, SAE, September 2003.
9. Gravel, R., and Mendler, C. (DOE, ENVERA): Variable Compression Ration (VCR) Engine, OAAT Accomplishments, [www.eere.energy.gov/vehiclesandfuels/pdfs/success/vcr3\\_29\\_01.pdf](http://www.eere.energy.gov/vehiclesandfuels/pdfs/success/vcr3_29_01.pdf)
10. European Commission, Community Research, Variable Compression Ratio Technology for CO<sub>2</sub> Reduction of Gasoline Engine Passenger Cars, [europa.eu.int/comm/research/conferences/2002/pdf/presspacks/1-1-vcr\\_en.pdf](http://europa.eu.int/comm/research/conferences/2002/pdf/presspacks/1-1-vcr_en.pdf)
11. Natj, Paul (GM): The Wall Street Journal Online and on page B1, Autos: Car Makers Seek New Spark In Gas Engines, September 28, 2004.
12. Greene, David L. (ORNL), Duleep, K.G. (EEA), McManus, Walter (J.D. Power and Associates): Future Potential of Hybrid and Diesel Powertrains in the U.S. Light-Duty Vehicle Market, Oak Ridge National Laboratory Pub ORNL/TM-2004/181, August 2004.
13. Road & Track Buyers Guide, 2006, page 36 Road & Track magazine.